Soft Matter

A Fluidic Demultiplexer for Controlling Large Arrays of Soft Actuators

Journal:	*Soft Matter*
Manuscript ID	SM-ART-12-2019-002502.R2
Article Type:	Paper
Date Submitted by the Author:	25-Mar-2020
Complete List of Authors:	Bartlett, Nicholas; Harvard University Becker, Kaitlyn; Harvard University Wood, Robert; Harvard University,

ARTICLE

A Fluidic Demultiplexer for Controlling Large Arrays of Soft Actuators

Nicholas W. Bartlett,[a] Kaitlyn P. Becker [a] and Robert J. Wood*[a]

Received 00th January 20xx,
Accepted 00th January 20xx

DOI: 10.1039/x0xx00000x

The field of soft robotics endeavors to create robots that are mostly, if not entirely, soft. While there have been significant advances in both soft actuators and soft sensors, there has been relatively little work done in the development of soft control systems. This work proposes a soft microfluidic demultiplexer as a potential control system for soft robotics. Demultiplexers enable the control of many outputs with just a few inputs, increasing a soft robot's complexity while minimizing its reliance on external valves and other off-board components. The demultiplexer in this work improves upon earlier microfluidic demultiplexers with its nearly two-fold reduction of inputs, a design feature that simplifies control and increases efficiency. Additionally, the demultiplexer in this work is designed to accommodate the high pressures and flow rates that soft robotics demands. The demultiplexer is characterized from the level of individual valves to full system parameters, and its functionality is demonstrated by controlling an array of individually addressable soft actuators.

Introduction

The field of soft robotics strives to create machines composed of soft, flexible materials, as opposed to the rigid, unyielding metals and hard plastics traditionally used in robotics. It has been argued that soft-bodied robots offer many advantages over their rigid counterparts, such as inherent safety in human-robot interactions through compliance matching, superior capabilities even with fewer control inputs via mechanical intelligence and morphological computation, reduced manufacturing costs and simpler fabrication, and overall increased robustness. [1-6]

With the promise of the above-mentioned benefits, the field of soft robotics has attracted much attention over the past decade.[7] Yet, a grand challenge of soft robotics is the demonstration of a fully soft, untethered, highly functional robot. The vast majority of fully soft robots are tethered, relying on off-board components for either power or control, or both.[8-13] Almost all untethered systems are not fully soft, as they incorporate rigid elements such as batteries, circuit boards, or mechanical valves.[14-18] The authors are aware of only one example of a fully soft, untethered robot: the Octobot.[19] While certainly an impressive demonstration of highly integrated fabrication, and a significant step forward for the field, the Octobot is only able to perform one preprogrammed motion. As such, the field is still in search of its first example of a fully soft, untethered robot capable of diverse behaviors.

Any autonomous robot has fundamental subsystems that include structure, actuation, sensing, power, and control. The structural subsystem is essentially the body of the robot, and ties together the other subsystems. The actuation subsystem is what enables the robot to move. Arguably the majority of research in soft robotics to date has been in developing muscle-like actuators; as such, there are many examples.[20-26] Most of these soft actuators are fluidic, in that they are powered either hydraulically or pneumatically. The sensing subsystem allows the robot to receive input from its environment. There are myriad demonstrations of soft sensors as well.[27-32] The power subsystem provides the energy with which the actuators perform work. Although research in this area has been overshadowed by developments in actuators and sensors, there are a number of power subsystems for soft robots.[33-35] The control subsystem is situated between the power and actuation subsystems (perhaps with input from the sensing subsystem, if there is feedback) to dictate how and when power is delivered to the actuators. Of all the subsystems, soft controllers are perhaps the least developed.[36]

Indeed, one of the central motivations for developing soft robots is that they exhibit a kind of mechanical intelligence in which the body or structure reacts organically to the environment, obviating the need for traditional control feedback loops that rely on precision sensing and actuation. However, even if feedback control may be deemed unnecessary in some (or even all) soft robots, the challenge of distributing energy to the system's actuators remains.

When implementing a control subsystem for a soft robot, robot designers must carefully consider the design of the full system. A majority of current soft actuators are powered by pressurized fluid; accordingly, fluidic control may be an appropriate choice for many soft robots. Using the same medium for the power, control, and actuation subsystems lends itself to more

[a] John A. Paulson School of Engineering and Applied Sciences, Harvard University, Cambridge, MA 02138.
* Corresponding author. Email: rjwood@seas.harvard.edu
Electronic Supplementary Information (ESI) available: [details of any supplementary information available should be included here]. See DOI: 10.1039/x0xx00000x

straightforward subsystem integration and overall simplicity. A single medium also allows the robot designer to blur the boundaries between various subsystems, enabling greater design freedom. This type of subsystem fluidity is much harder (or potentially impossible) to accomplish with mismatched media. While traditional control subsystems are electrical (e.g., microcontrollers and computers), there are applications in which we may want to avoid electricity, such as in robots that operate underwater. Additionally, there are many situations in which we may want to offload as much low-level control to the mechanics of a system as possible. Finally, a fluidic control subsystem may be composed of microfluidic valves that are significantly smaller and less expensive than the electromechanical solenoid valves that are typically used to interface between an electrical control subsystem and a fluidic actuation subsystem.

Given that not all subsystems have been developed at the same rate, many soft robots are tethered to allow off-board power and control. Tethered systems may be seen as stepping stones to future untethered robots or as final systems in their own right. Regardless, we should still seek to minimize the influence of tethers on the behavior of the system. That is, we should strive for small tethers with as few lines as possible over large, obtrusive tethers composed of many lines. A physically large tether may pull on a robot, introducing undesirable forces and moments. Furthermore, abrupt changes in mechanical properties at interfaces are a common source of failure in soft robotics; as such, a complex tether that relies on many parallel, independent connections will be significantly less robust than a simpler tether with only a few connections.[15, 37]

In this work, we propose that the functionality of soft robots may be enhanced through a soft control subsystem that exploits microfluidic multiplexing. A demultiplexer enables control over a large number of outputs with only a few inputs, and can be seamlessly embedded within the body of a soft robot itself. Such a control architecture minimizes the size and complexity of any tether by drastically reducing the number of control lines required to address all of the robot's actuators. By moving more of the control subsystem on-board, microfluidic multiplexing brings the field closer to fully soft, untethered, highly functional robots.

Demultiplexer

A demultiplexer is a device that allows a small number of control inputs to select one among a much greater number of outputs (see Fig. 1A). Each input toggles the state of every output, ensuring that half of the outputs are open and half of the outputs are closed (see Fig. 1B). The first input ensures inverse states for the first and second halves of the outputs. The second input again ensures inverse states for half of the outputs, but does so by keeping the first and third quarters of the outputs in the inverse state of the second and fourth quarters. Later inputs select smaller and smaller groupings of outputs (eighths, sixteenths, thirty-seconds, etc.) until the groupings consists of single alternating outputs. By selecting which half of the outputs are controlled by a given input, n outputs can be controlled with just $log_2 n$ inputs. This scaling has been demonstrated repeatedly in the electrical domain.

The demultiplexer presented in this work closely follows earlier designs in the microfluidics literature, but with notable and important differences.[38] In that earlier work, each input was actually two independent microfluidic channels which were externally constrained to be in inverse pressurization states. That is, while one was pressurized, the other was manually depressurized. As such, the number of inputs required to control n outputs was shown to be $2log_2 n$.

The multiplexing scheme in this work more closely resembles the scaling laws of the electrical domain in that the number of inputs required to control n outputs is just $log_2 n+2$. We accomplish this nearly two-fold reduction in the number of required control inputs compared to previously reported microfluidic demultiplexers by explicitly enforcing the inverse pressurization state requirement in the demultiplexer itself rather than doing so artificially through external manipulation. The fundamental difference is a single line that acts as both a flow channel and a control channel simultaneously. While another microfluidic demultiplexer with more favorable scaling has been demonstrated previously, that demultiplexer requires the introduction of a vacuum control channel in addition to a pressure control channel, which fundamentally limits the maximum pressure that can be delivered to the actuators.[39]

Referring to Fig. 1B, the outputs $O_0 – O_7$ are all connected to a single input channel on the flow layer, denoted “Flow” (*F*). This channel is set to a predetermined pressure (P_F), and is only depressurized when switching between outputs. A separate network of interconnected channels on the flow layer is connected to a distinct input, denoted “Primary Control” (*PC*). The input to this line is also set to a predetermined pressure (P_{PC}, with $P_{PC} > P_F$), and again is only depressurized when switching between outputs. Each branch of *PC* transitions from the flow layer to the control layer by means of microfluidic vias (depicted as circles in Fig. 1B). The continuation of these channels on the control layer (PC_2, PC_1, and PC_0) then cross under the output channels of the *F* line ($O_0 – O_7$). Where their widths increase, these channels behave as valves; where their widths remain small, these channels do not affect the flow of the channels above them. Finally, there are the channels denoted “Secondary Control” (*SC*), each of which may be toggled between atmospheric pressure and a given high pressure (P_{SC}, with $P_{SC} > P_{PC}$). That is, some *SC* channels may be depressurized when selecting a given output. Each *SC* channel features a set of valves that toggles half of the outputs, but also features an additional valve that closes a branch of the *PC* channel, opening the other half of the outputs.

It should be appreciated that the input channels must be pressurized and depressurized in a particular order to avoid creating air pockets within the demultiplexer. Beginning with a

fully depressurized demultiplexer, the desired *SC* channels are pressurized first, followed by the *PC* channel, and finally the *F* channel, thereby pressurizing the selected output. Before selecting a new output, the inputs must be depressurized in the reverse sequence to again fully depressurize the demultiplexer. (Additional details can be found in the supplementary information.)

Considering the three (secondary) input, eight output demultiplexer in Fig. 1B, the default state is all inputs low, corresponding to [SC_2 SC_1 SC_0] = [0 0 0]. In this state, PC_2 closes $O_4 - O_7$, PC_1 closes O_2, O_3, O_6, and O_7, and PC_0 closes O_1, O_3, O_5, and O_7. Consequently, O_0 is selected. If SC_0 is set high (giving [0 0 1] for the input state), the first valve on SC_0 closes PC_0, such that O_1, O_3, O_5, and O_7 are no longer closed (at least, not by PC_0). Downstream, SC_0 closes O_0, O_2, O_4, and O_6. Consequently, O_1 is selected. Any output may be selected with the correct combination of secondary inputs. In fact, the input state vector [SC_2 SC_1 SC_0] is exactly the selected output in binary notation (e.g., [101] selects O_5). A fully functional demultiplexer can be viewed in Movie S1.

Valve Design and Characterization

At the heart of any demultiplexer is a switch that can toggle an output between two states: on or off, open or closed. In electronics, that switch is a transistor that toggles between a low voltage and a high voltage. In microfluidics, that switch is a valve that either stops flow in a microchannel, or allows flow to proceed uninhibited. The microfluidic valve presented in this paper is an adaptation of the first microfluidic valve presented by Unger et al.[40] While other novel soft valves have been presented, their size, geometry, and fabrication process do not scale well to allow the number of valves required for a multiplexing scheme.[41, 42] A traditional microfluidic valve consists of two perpendicularly oriented microchannels, offset slightly in the vertical direction so that they are separated by a thin membrane (see Fig. 2A). When one microchannel is pressurized, it expands, deforming the surrounding elastomer, and causing the membrane to deflect into the other microchannel, impeding the flow (see Fig. 2B). We call the "flow" channel the microchannel that carries the fluid whose flow is modulated by the valve, and we call the "control" channel the microchannel whose pressurization closes the valve. In our configuration, the control channel is always below the flow channel, in a configuration called a "push-up" valve. Others have shown that, under certain assumptions, this configuration is preferable to the alternative "push-down" configuration, in which the control channel is above the flow channel.[43] We have shown previously that the shape of the flow channel is critical to ensure full valve closure, and that various fabrication strategies may be employed to achieve acceptable channel shapes, subject to a wide array of design requirements.[44] In this work, we fabricate microchannel molds using both 3D printing and soft lithography (details can be found in the supplementary information).

Analytical models of microfluidic valves have been presented in the literature.[43, 45] However, these models make assumptions about the profile of the flow channel that do not apply to the valves presented here (e.g., that the profile is parabolic). Modifying these analytical models to accommodate our valve geometry would quickly become intractable. As such, we opted to characterize our valves experimentally.

Valve characterization consisted of a variable sweep of channel sizes and membrane thicknesses. By systematically altering individual variables, we determined the control pressure (P_c) required to stop a given flow pressure (P_f) as a function of control channel width (w_c), flow channel width (w_f), and membrane thickness (m) (see Figs. 2A and 2B; more details can be found in the supplementary information). We found that, while the widths of the flow and control channels have a slight effect on the valve closing pressure, the membrane thickness more strongly influences valve behavior (see Fig. 2C). This decoupling is fortuitous in that system requirements (such as actuator pressure and actuation frequency) can drive channel geometry while valve behavior can be tuned simply by altering the membrane thickness.

Due to the strong influence of the membrane on valve behavior, we sought to understand the contribution from material choice in addition to geometry. While most microfluidic systems are fabricated from Sylgard 184 (Dow Corning), we found this material to be functionally limited, especially in that it is a relatively stiff elastomer, with a Shore durometer of 43.8A.[46] We investigated the use of an alternate elastomer, MED4-4220 (NuSil Technology), which has a Shore durometer of 17A.[47, 48] While preliminary valve testing was done with membranes made from Sylgard 184, we repeated the characterization described above with membranes made from MED4-4220 and found that otherwise identical valves actuated at smaller pressure differences and survived more actuation cycles.

Actuator Design and Fabrication

The demultiplexer discussed above has been designed to operate at a scale large enough to be relevant to soft robotics. The test of such a system is in its ability to operate functional actuators; for such a demonstration, we have chosen to use tri-chambered pneumatic bending actuators.[49] While the demultiplexer presented here could be adapted to any of a wide variety of soft fluidic actuators, we have specifically chosen these actuators for three reasons. First, the actuators are small enough that we can fabricate a large array in a small area, demonstrating the favorable scaling properties of the demultiplexer. Second, we are able to show complex motions to mirror the non-trivial microfluidic logic scheme, because the actuators each possess two degrees of freedom. Finally, we demonstrate one fabrication strategy for integration of actuation and control subsystems by using both molding and soft lithographic techniques.

Each actuator consists of three individually addressable pneumatic chambers. Because each chamber is offset from the neutral axis of the actuator, pressurizing any one chamber produces a moment which causes the actuator to bend. By modulating the pressure in each chamber, one can produce bending in any direction. Fig. 3 depicts the typical bending modes of the actuator, as does Movie S2.

An actuator is fabricated by dip-coating uncured elastomer onto a set of three pins which are press-fit into a custom laser-cut fixture. The first dip-coat covers the individual pins with elastomer. Further dippings continue to coat the individual pins, but also allow elastomer to bridge between the pins, forming a single tri-chambered actuator. More details on the fabrication process can be found in the supplementary information.

Integrated Demultiplexer and Soft Actuator Array

To integrate the demultiplexer with an array of actuators, we had to address system-level concerns. The actuators exhibit a trade-off in that fewer coatings during fabrication enable a lower actuation pressure, but also pose a higher risk of failure due to a defect in a thin chamber wall. In a large array in which a single failed actuator would compromise the entire system, we prioritized robustness over a lower operating pressure.

To develop the integrated system, very few modifications to the fabrication procedure were necessary. Whereas the actuators were previously made by coating pins that were directly press-fit into their acrylic fixture, in the integrated system we inserted the pins through the top layer of the demultiplexer before they were inserted into the fixture. In this way, the elastomer that would form the actuators would drip down the pins and coat the surface of the demultiplexer as it was curing, forming a conformal seal. Once the actuators were cured, the pins were removed from the back of the top demultiplexer layer, which was then plasma bonded to the remaining demultiplexer layers.

In contrast to the demultiplexer schematics in Fig. 1, we demonstrate a fully integrated system with a 4 (secondary) input, 16 output demultiplexer. In this demonstration (see Fig. 4 and Movie S3), five tri-chambered actuators are arranged at the vertices of a pentagon (in this system, only 15 of the available 16 outputs are used). In this configuration, we can demonstrate both clockwise and counter clockwise actuation sequences, in addition to an outward radial actuation sequence. Although only a single output can be addressed at a time, simultaneous control of multiple outputs may be approximated by quickly cycling through the inputs, up to the limits imposed by the pressure levels of the system and the actuator dynamics.

Conclusions

Many advances in the field of soft robotics have revolved around sensors and actuators. Developments in soft control subsystems, in contrast, have been greatly limited. In this work, we propose a microfluidic multiplexing architecture that suggests one possible path forward for soft control systems.

While microfluidic multiplexing has been demonstrated previously, there are three distinct differences presented in this work. First, we use a multiplexing scheme that much more closely resembles the architecture of electrical demultiplexers, decreasing the number of required control channels by a factor of two compared to earlier publications. We are able to demonstrate such drastic reductions by taking advantage of the shared media (i.e., fluid) between the actuation and control subsystems, a feat that would be much more challenging with mixed media subsystems (e.g., fluid actuation and electrical control). Second, the size of the system is scaled to be able to accommodate much higher pressures and flow rates, bringing microfluidic multiplexing into relevance for soft robotics. Finally, we introduce a new membrane material to accommodate the higher pressures and flow rates required in a scaled-up system.

We demonstrate the functionality and applicability of our demultiplexer by controlling an array of tri-chambered actuators. Beyond this demonstration, we anticipate that such a multiplexing scheme will be highly relevant for tethered soft robotic systems that seek to minimize the effect of a tether. For example, microfluidic multiplexing may be appealing to surgeons who need to control a large number of degrees of freedom in a laparoscopic tool, and yet only have a limited size laparoscopic port for the tether.

Conflicts of interest

There are no conflicts to declare.

Acknowledgements

This work was supported by the Wyss Institute for Biologically Inspired Engineering and the Office of Naval Research (award #N00014-17-1-2063). N.W.B. was supported by the Army Research Office, National Defense Science and Engineering Graduate (NDSEG) Fellowship and K.P.B was supported by the National Science Foundation Graduate Research Fellowship (under grant DGE1144152). Any opinions, findings, conclusions, or recommendations expressed in this material are those of the authors and do not necessarily reflect those of the funding organizations.

Notes and references

1 D. Trivedi, C. D. Rahn, W. M. Kier, and I. D. Walker, “Soft robotics: Biological inspiration, state of the art, and future research,” Applied bionics and biomechanics, vol. 5, no. 3, pp. 99–117, 2008.
2 S. Kim, C. Laschi, and B. Trimmer, “Soft robotics: a bioinspired

evolution in robotics,"Trends in biotechnology, vol. 31, no. 5, pp. 287–294, 2013.
3 C. Majidi, "Soft robotics: a perspective—current trends and prospects for the future," Soft Robotics, vol. 1, no. 1, pp. 5–11, 2014.
4 D. Rus and M. T. Tolley, "Design, fabrication and control of soft robots," Nature, vol. 521, no. 7553, p. 467, 2015.
5 C. Laschi, B. Mazzolai, and M. Cianchetti, "Soft robotics: Technologies and systems pushing the boundaries of robot abilities," Sci. Robot., vol. 1, no. 1, p. eaah3690, 2016.
6 P. Polygerinos, N. Correll, S. A. Morin, B. Mosadegh, C. D. Onal, K. Petersen, M. Cianchetti, M. T. Tolley, and R. F. Shepherd, "Soft robotics: Review of fluid-driven intrinsically soft devices; manufacturing, sensing, control, and applications in human-robot interaction," Advanced Engineering Materials, 2017.
7 G. Bao, H. Fang, L. Chen, Y. Wan, F. Xu, Q. Yang, and L. Zhang, "Soft robotics: Academic insights and perspectives through bibliometric analysis," Soft robotics, 2018.
8 R. F. Shepherd, F. Ilievski, W. Choi, S. A. Morin, A. A. Stokes, A. D. Mazzeo, X. Chen, M. Wang, and G. M. Whitesides, "Multigait soft robot," Proceedings of the national academy of sciences, vol. 108, no. 51, pp. 20400–20403, 2011.
9 R. F. Shepherd, A. A. Stokes, J. Freake, J. Barber, P. W. Snyder, A. D. Mazzeo, L. Cademartiri, S. A. Morin, and G. M. Whitesides, "Using explosions to power a soft robot," Angewandte Chemie, vol. 125, no. 10, pp. 2964–2968, 2013.
10 C. Christianson, N. N. Goldberg, D. D. Deheyn, S. Cai, and M. T. Tolley, "Translucent soft robots driven by frameless fluid electrode dielectric elastomer actuators," Science Robotics, vol. 3, no. 17, p. eaat1893, 2018.
11 S. Song, D.-M. Drotlef, C. Majidi, and M. Sitti, "Controllable load sharing for soft adhesive interfaces on three-dimensional surfaces," Proceedings of the National Academy of Sciences, p. 201620344, 2017.
12 A. Rafsanjani, Y. Zhang, B. Liu, S. M. Rubinstein, and K. Bertoldi, "Kirigami skins make a simple soft actuator crawl," Science Robotics, vol. 3, no. 15, p. eaar7555, 2018.
13 T. Ranzani, S. Russo, N. W. Bartlett, M. Wehner, and R. J. Wood, "Increasing the dimensionality of soft microstructures through injection-induced self-folding," Advanced Materials, p. 1802739, 2018.
14 M. T. Tolley, R. F. Shepherd, B. Mosadegh, K. C. Galloway, M. Wehner, M. Karpelson, R. J. Wood, and G. M. Whitesides, "A resilient, untethered soft robot," Soft robotics, vol. 1, no. 3, pp. 213–223, 2014.
15 N. W. Bartlett, M. T. Tolley, J. T. Overvelde, J. C. Weaver, B. Mosadegh, K. Bertoldi, G. M. Whitesides, and R. J. Wood, "A 3d-printed, functionally graded soft robot powered by combustion," Science, vol. 349, no. 6244, pp. 161–165, 2015.
16 A. D. Marchese, C. D. Onal, and D. Rus, "Autonomous soft robotic fish capable of escape maneuvers using fluidic elastomer actuators," Soft Robotics, vol. 1, no. 1,pp. 75–87, 2014.
17 C. D. Onal and D. Rus, "Autonomous undulatory serpentine locomotion utilizing body dynamics of a fluidic soft robot," Bioinspiration & biomimetics, vol. 8, no. 2,p. 026003, 2013.
18 J. Cao, L. Qin, H. P. Lee, and J. Zhu, "Development of a soft untethered robot using artificial muscle actuators," in Electroactive Polymer Actuators and Devices (EAPAD)2017, vol. 10163, p. 101631X, International Society for Optics and Photonics, 2017.
19 M. Wehner, R. L. Truby, D. J. Fitzgerald, B. Mosadegh, G. M. Whitesides, J. A. Lewis, and R. J. Wood, "An integrated design and fabrication strategy for entirely soft, autonomous robots," Nature, vol. 536, no. 7617, p. 451, 2016.
20 B. Mosadegh, P. Polygerinos, C. Keplinger, S. Wennstedt, R. F. Shepherd, U. Gupta,J. Shim, K. Bertoldi, C. J. Walsh, and G. M. Whitesides, "Pneumatic networks for soft robotics that actuate rapidly," Advanced functional materials, vol. 24, no. 15,pp. 2163–2170, 2014.
21 F. Ilievski, A. D. Mazzeo, R. F. Shepherd, X. Chen, and G. M. Whitesides, "Soft robotics for chemists," Angewandte Chemie, vol. 123, no. 8, pp. 1930–1935, 2011.
22 S. Li, D. M. Vogt, D. Rus, and R. J. Wood, "Fluid-driven origami-inspired artificial muscles," Proceedings of the National Academy of Sciences, p. 201713450, 2017.
23 D. Yang, M. S. Verma, J.-H. So, B. Mosadegh, C. Keplinger, B. Lee, F. Khashai, E. Lossner, Z. Suo, and G. M. Whitesides, "Buckling pneumatic linear actuators inspired by muscle," Advanced Materials Technologies, vol. 1, no. 3, 2016.
24 L. Hines, K. Petersen, G. Z. Lum, and M. Sitti, "Soft actuators for small-scale robotics," Advanced Materials, vol. 29, no. 13, 2017.
25 S. Seok, C. D. Onal, K.-J. Cho, R. J. Wood, D. Rus, and S. Kim, "Meshworm: a peristaltic soft robot with antagonistic nickel titanium coil actuators," IEEE/ASME Transactions on mechatronics, vol. 18, no. 5, pp. 1485–1497, 2013.
26 S. Shian, K. Bertoldi, and D. R. Clarke, "Dielectric elastomer based "grippers" for soft robotics," Advanced Materials, vol. 27, no. 43, pp. 6814–6819, 2015.
27 D. M. Vogt, Y.-L. Park, and R. J. Wood, "Design and characterization of a soft multi-axis force sensor using embedded microfluidic channels," IEEE sensors Journal, vol. 13, no. 10, pp. 4056–4064, 2013.
28 C. Larson, B. Peele, S. Li, S. Robinson, M. Totaro, L. Beccai, B. Mazzolai, and R. Shepherd, "Highly stretchable electroluminescent skin for optical signaling and tactile sensing," Science, vol. 351, no. 6277, pp. 1071–1074, 2016.
29 C.-C. Kim, H.-H. Lee, K. H. Oh, and J.-Y. Sun, "Highly stretchable, transparent ionic touch panel," Science, vol. 353, no. 6300, pp. 682–687, 2016.
30 J. Kim, G. A. Salvatore, H. Araki, A. M. Chiarelli, Z. Xie, A. Banks, X. Sheng, Y. Liu, J. W. Lee, K.-I. Jang, et al., "Battery-free, stretchable optoelectronic systems for wireless optical characterization of the skin," Science advances, vol. 2, no. 8,p. e1600418, 2016.
31 Y. Gao, H. Ota, E. W. Schaler, K. Chen, A. Zhao, W. Gao, H. M. Fahad, Y. Leng, A. Zheng, F. Xiong, et al., "Wearable microfluidic diaphragm pressure sensor for health and tactile touch monitoring," Advanced Materials, vol. 29, no. 39, 2017.
32 N. Lu and D.-H. Kim, "Flexible and stretchable electronics paving the way for soft robotics," Soft Robotics, vol. 1, no. 1, pp. 53–62, 2014.
33 C. Stergiopulos, D. Vogt, M. T. Tolley, M. Wehner, J. Barber, G. M. Whitesides, and R. J. Wood, "A soft combustion-driven pump for soft robots," in ASME 2014 Conference on Smart Materials, Adaptive Structures and Intelligent Systems, pp. V002T04A011–V002T04A011, American Society of Mechanical Engineers, 2014.
34 M. Wehner, M. T. Tolley, Y. Menguc, Y.-L. Park, A. Mozeika, Y. Ding, C. Onal, R. F. Shepherd, G. M. Whitesides, and R. J. Wood, "Pneumatic energy sources for autonomous and wearable soft robotics," Soft Robotics, vol. 1, no. 4, pp. 263–274, 2014.
35 C. D. Onal, X. Chen, G. M. Whitesides, and D. Rus, "Soft mobile robots with on-board chemical pressure generation," in Robotics Research, pp. 525–540, Springer,2017.
36 B. Trimmer, "Soft robot control systems: A new grand challenge?," 2014.
37 Y. Menguc, Y.-L. Park, H. Pei, D. Vogt, P. M. Aubin, E. Winchell, L. Fluke, L. Stirling, R. J. Wood, and C. J. Walsh, "Wearable soft sensing suit for human gait measurement," The International Journal of Robotics Research, vol. 33, no. 14,pp. 1748–1764, 2014.

38 T. Thorsen, S. J. Maerkl, and S. R. Quake, "Microfluidic large-scale integration," Science, vol. 298, no. 5593, pp. 580–584, 2002.
39 W. H. Grover, R. H. Ivester, E. C. Jensen, and R. A. Mathies, "Development and multiplexed control of latching pneumatic valves using microfluidic logical structures," Lab on a Chip, vol. 6, no. 5, pp. 623–631, 2006.
40 M. A. Unger, H.-P. Chou, T. Thorsen, A. Scherer, and S. R. Quake, "Monolithic microfabricated valves and pumps by multilayer soft lithography," Science, vol. 288, no. 5463, pp. 113–116, 2000.
41 P. Rothemund, A. Ainla, L. Belding, D. J. Preston, S. Kurihara, Z. Suo, and G. M. Whitesides, "A soft, bistable valve for autonomous control of soft actuators," Science Robotics, vol. 3, no. 16, p. eaar7986, 2018.
42 D. J. Preston, P. Rothemund, H. J. Jiang, M. P. Nemitz, J. Rawson, Z. Suo, and G. M. Whitesides, "Digital logic for soft devices," Proceedings of the National Academy of Sciences, p. 201820672, 2019.
43 P. Fordyce, C. Diaz-Botia, J. DeRisi, and R. Gomez-Sjoberg, "Systematic characterization of feature dimensions and closing pressures for microfluidic valves produced via photoresist reflow," Lab on a Chip, vol. 12, no. 21, pp. 4287–4295, 2012.
44 N. W. Bartlett and R. J. Wood, "Comparative analysis of fabrication methods for achieving rounded microchannels in PDMS," Journal of Micromechanics and Microengineering, vol. 26, no. 11, p. 115013, 2016.
45 E. P. Kartalov, A. Scherer, S. R. Quake, C. R. Taylor, and W. F. Anderson, "Experimentally validated quantitative linear model for the device physics of elastomeric microfluidic valves," Journal of applied physics, vol. 101, no. 6, p. 064505, 2007.
46 I. Johnston, D. McCluskey, C. Tan, and M. Tracey, "Mechanical characterization of bulk sylgard 184 for microfluidics and microengineering,"Journal of Micromechanics and Microengineering, vol. 24, no. 3, p. 035017, 2014.
47 NuSil Technology, MED4-4220 Data Sheet, 7 2018. https://nusil.com/services/downloadfile.ashx?productcode=MED4-4220&originalname=MED4-4220.pdf.
48 S. Russo, T. Ranzani, C.J. Walsh, and R. J. Wood, "An Additive Millimeter-Scale Fabrication Method for Soft Biocompatible Actuators and Sensors," Advanced Materials Technologies, vol. 2, no. 10, p. 1700135, 2017.
49 K. Suzumori, S. Iikura, and H. Tanaka, "Development of flexible microactuator and its applications to robotic mechanisms," in Proceedings. 1991 IEEE International Conference on Robotics and Automation, pp. 1622–1627, IEEE, 1991.
50 K. P. Becker, Y. Chen, and R. J. Wood, "Mechanically Programmable Dip Molding of High Aspect Ratio Soft Actuator Arrays," Advanced Functional Materials, p. 1908919, 2020.

Figure captions

Figure 1: Demultiplexer design schematic. (A) In this work, we use a demultiplexer to reduce the number of control lines required to address a soft actuator array. Generally, a demultiplexer uses n inputs to select one among 2^n outputs. **(B)** *F* and *PC* lines are always pressurized when an output is selected, with the pressure of the *PC* line greater than that of the *F* line. The three *SC* lines may either be pressurized (to a pressure greater than that of the *PC* line) or vented to atmospheric pressure to select among the eight outputs. This example design demonstrates control of eight outputs with three secondary inputs (plus one primary input). *F*: Flow, *PC*: Primary Control, *SC*: Secondary Control, *O*: Output.

Figure 2: Principle of operation of a microfluidic valve. (A) A valve consists of two perpendicular microchannels offset slightly in the vertical direction. When the "flow" channel (blue) is above the "control" channel (pink), the valve is designated as "push-up". w_f: width of flow channel. w_c: width of control channel. **(B)** The top schematic shows a valve in an open state, whereas the bottom schematic shows a valve in a closed state. As the control channel is pressurized, it expands, deflecting the elastomeric membrane into the flow channel. P_c: pressure of control channel. m: membrane thickness. **(C) Valve characterization.** For four different membrane thicknesses (112, 105, 77, and 54 micrometers, corresponding to the gray, pink, purple, and green markers, respectively), we characterize the average difference in pressure between the control channel and the flow channel required to close the valve (i.e., mean ($P_c - P_f$)) as a function of the difference in channel width between the control channel and the flow channel (i.e., $w_c - w_f$). P_f: pressure of flow channel. Membrane material is MED4-4220 for the above data.

Figure 3: (A) Actuator principle of operation. A single actuator consists of three chambers. When any single chamber is inflated, the actuator bends towards the side of the actuator opposite the pressurized chamber. (The tops of the actuators are cut away in the image to show the individual chambers.) **(B) Actuator bending.** *Top left*: No chambers are pressurized, yielding an undeformed state. *Top right*: The front left chamber is pressurized, causing bending towards the back right. *Bottom left*: The front right chamber is pressurized, causing bending towards the back left. *Bottom right*: The back chamber is pressurized, causing bending towards the front.

Figure 4: Multiplexed soft actuator array. (A) A tri-chambered actuator is located at each vertex of a pentagon, aligned so that the actuator can bend along the edge of the pentagon. **(B)** Sequential actuation of the five tri-chambered actuators allows clockwise, counter clockwise, and radial actuation patterns. **(C)** Images of the fabricated pentaradial array during the first three states of a clockwise actuation sequence.

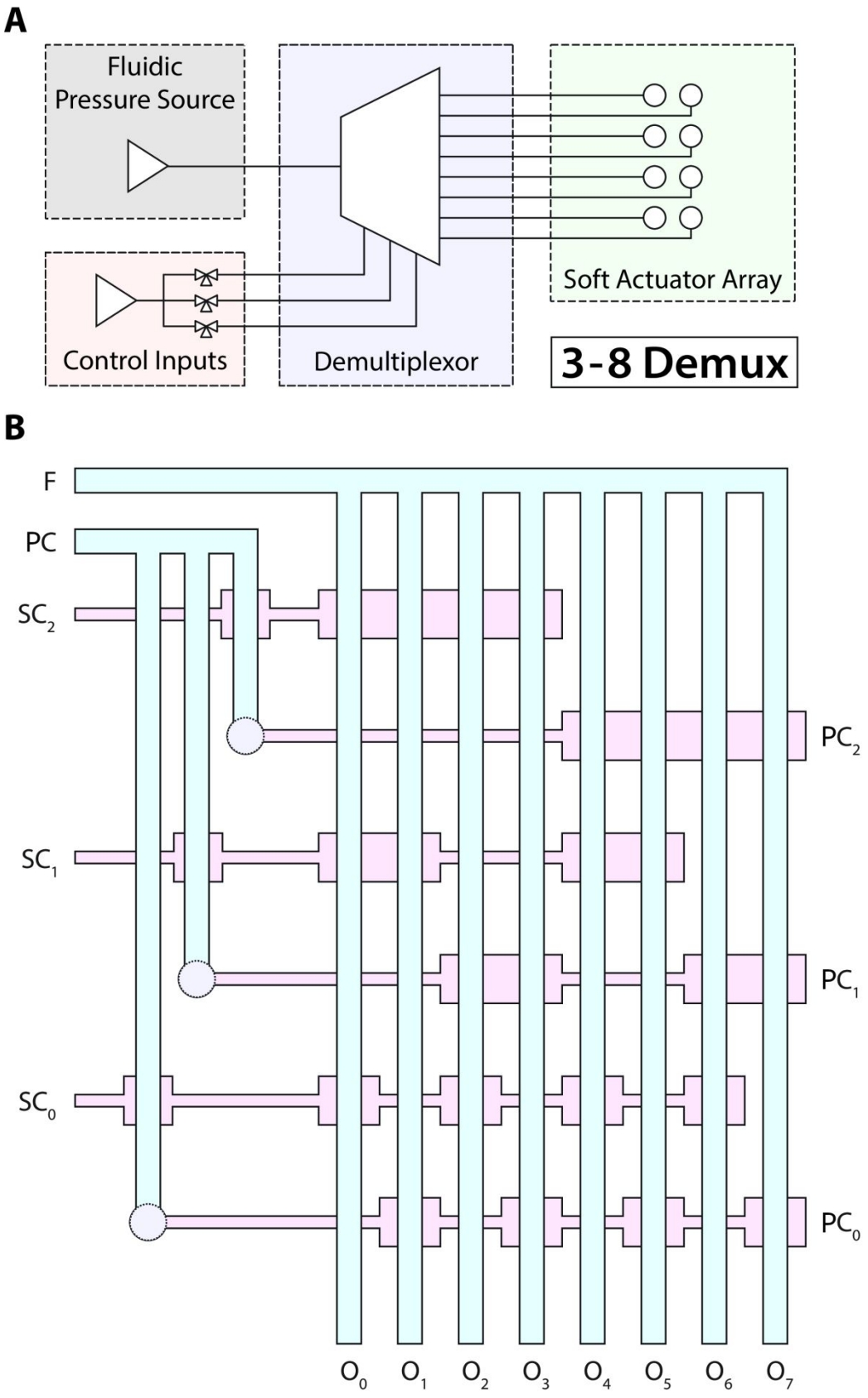
A
Fluidic
Pressure Source
Control Inputs
Demultiplexor
Soft Actuator Array
3-8 Demux
B
F
PC
SC2
SC1
SC0
PC2
PC1
PC0
O0
O1
O2
O3
O4
O5
O6
O7

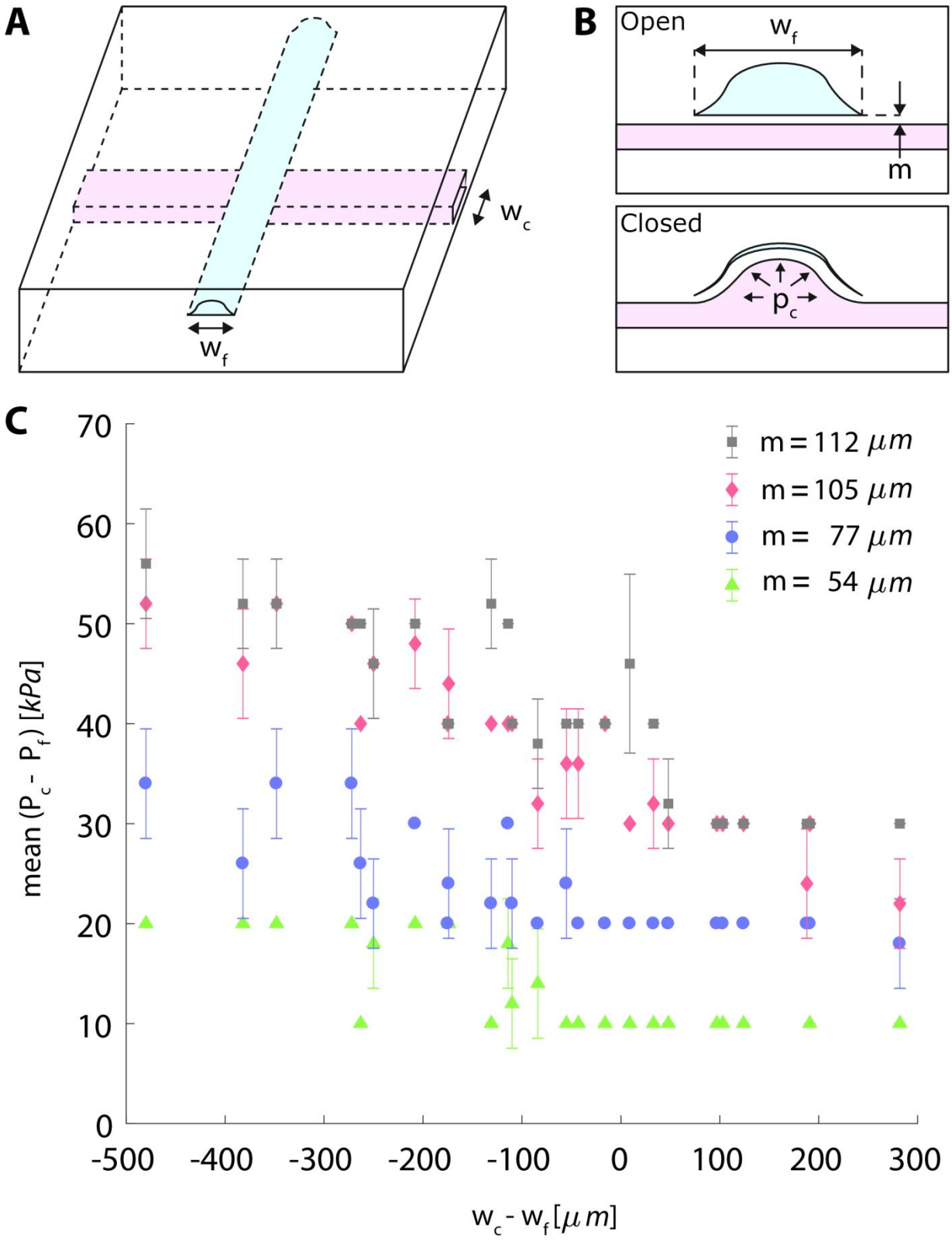
A
w_c
w_f
B
Open
w_f
m
Closed
p_c
C
m = 112 μm
m = 105 μm
m = 77 μm
m = 54 μm
mean (P_c - P_f) [kPa]
w_c - w_f [μm]
70
60
50
40
30
20
10
0
-500
-400
-300
-200
-100
0
100
200
300

A

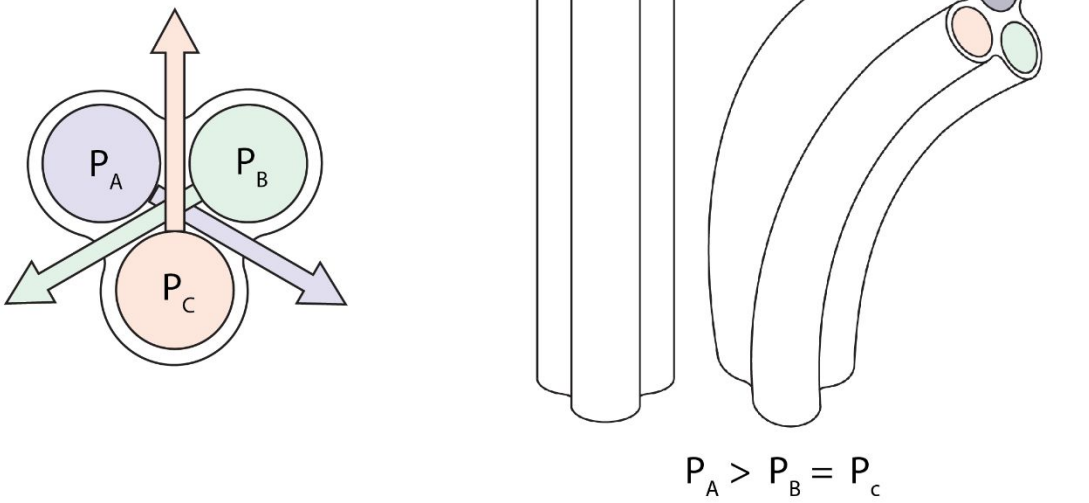

B

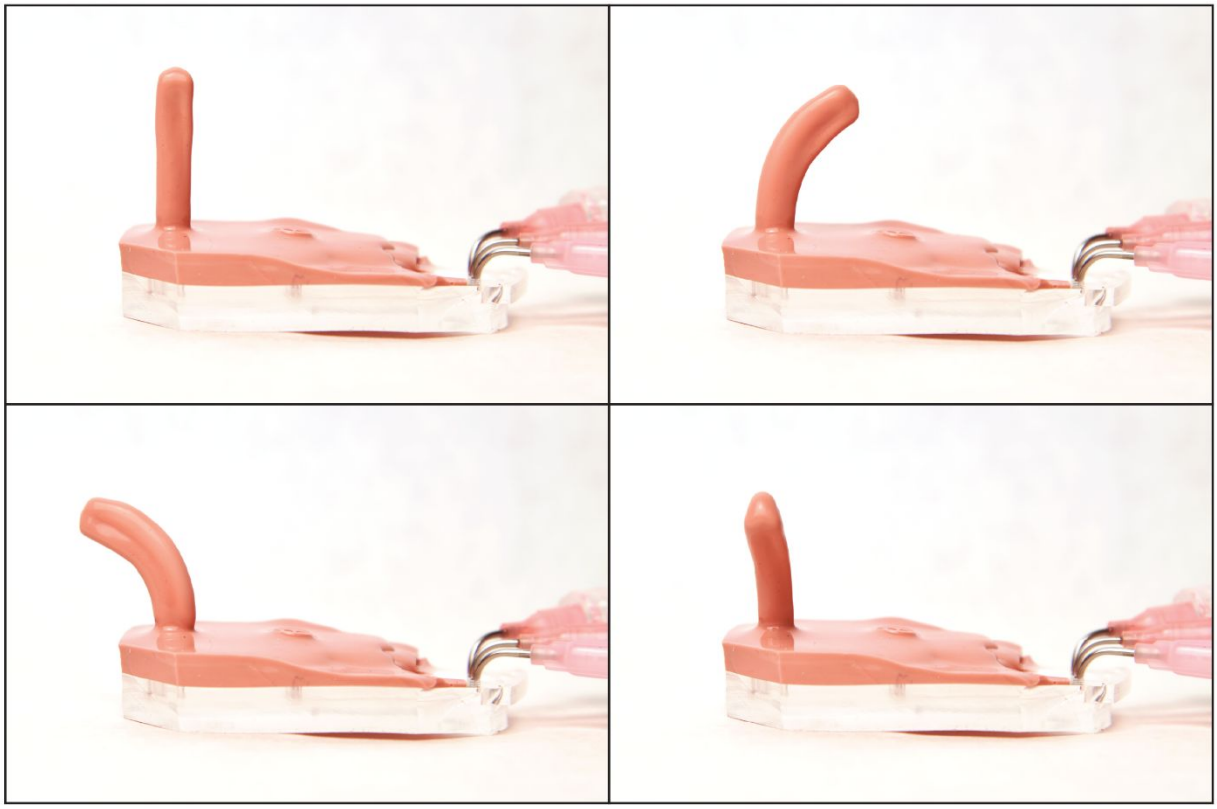

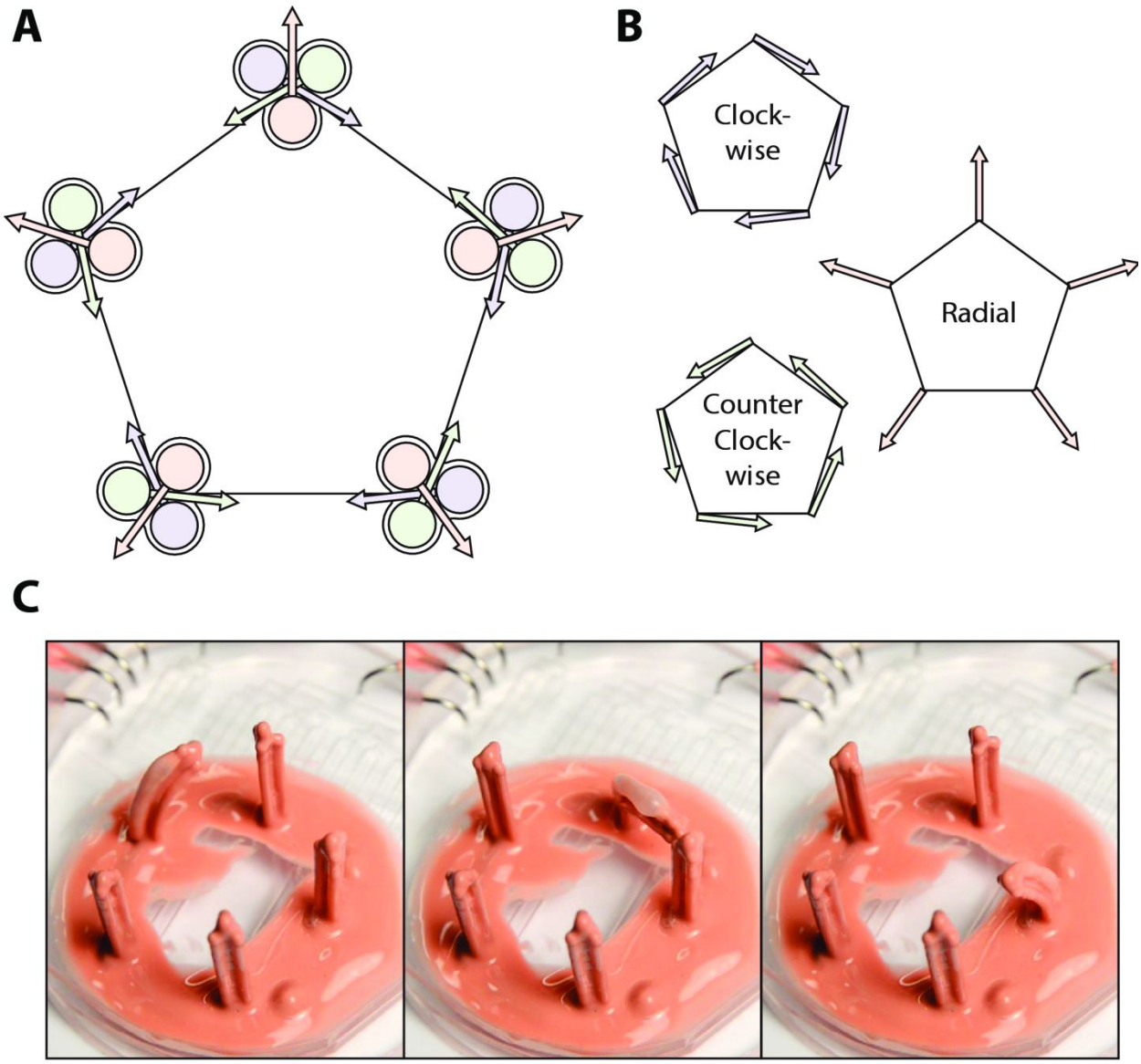
A
B
Clock-
wise
Radial
Counter
Clock-
wise
C

This work proposes a soft microfluidic demultiplexer as a potential control system for soft robotics.